EUROPEAN ORGANISATION FOR NUCLEAR RESEARCH

CERN-PPE/92-66
29 April 1992

Measurement of the τ Topological Branching Ratios at LEP

The OPAL Collaboration

Abstract

The inclusive branching ratios of the τ lepton to one, three and five charged particle final states are measured from data collected with the OPAL detector at LEP. The data sample consists of 12707 $e^+e^- \to \tau^+\tau^-$ candidate events and has an estimated background of 1.9%. The branching ratios are obtained from a simultaneous fit to the data which gives $B_1 = 84.48 \pm 0.27(stat) \pm 0.23(sys)\%$, $B_3 = 15.26 \pm 0.26 \pm 0.22\%$ and $B_5 = 0.26 \pm 0.06 \pm 0.05\%$ respectively, where $B_1 + B_3 + B_5$ is constrained to equal one. The inclusive one-prong branching ratio is found to be significantly lower than the 1990 Particle Data Group world average value while the branching ratio to three charged particles is correspondingly higher. The five-prong branching ratio is in agreement with the world average measurement.

(Submitted to Physics Letters B)

The OPAL Collaboration

P.D. Acton[25], G. Alexander[23], J. Allison[16], P.P. Allport[5], K.J. Anderson[9], S. Arcelli[2], A. Astbury[28], D. Axen[29], G. Azuelos[18,a], G.A. Bahan[16], J.T.M. Baines[16], A.H. Ball[17], J. Banks[16], G.J. Barker[13], R.J. Barlow[16], S. Barnett[16], J.R. Batley[5], G. Beaudoin[18], A. Beck[23], J. Becker[10], T. Behnke[27], K.W. Bell[20], G. Bella[23], P. Berlich[10], S. Bethke[11], O. Biebel[3], U. Binder[10], I.J. Bloodworth[1], P. Bock[11], B. Boden[3], H.M. Bosch[11], S. Bougerolle[29], H. Breuker[8], R.M. Brown[20], R. Brun[8], A. Buijs[8], H.J. Burckhart[8], P. Capiluppi[2], R.K. Carnegie[6], A.A. Carter[13], J.R. Carter[5], C.Y. Chang[17], D.G. Charlton[8], P.E.L. Clarke[25], I. Cohen[23], W.J. Collins[5], J.E. Conboy[15], M. Cooper[22], M. Couch[1], M. Coupland[14], M. Cuffiani[2], S. Dado[22], G.M. Dallavalle[2], S. De Jong[8], L.A. del Pozo[5], M.M. Deninno[2], A. Dieckmann[11], M. Dittmar[4], M.S. Dixit[7], E. do Couto e Silva[12], J.E. Duboscq[8], E. Duchovni[26], G. Duckeck[11], I.P. Duerdoth[16], D.J.P. Dumas[6], P.A. Elcombe[5], P.G. Estabrooks[6], E. Etzion[23], H.G. Evans[9], F. Fabbri[2], M. Fincke-Keeler[28], H.M. Fischer[3], D.G. Fong[17], C. Fukunaga[24,b], A. Gaidot[21], O. Ganel[26], J.W. Gary[4], J. Gascon[18], R.F. McGowan[16], N.I. Geddes[20], C. Geich-Gimbel[3], S.W. Gensler[9], F.X. Gentit[21], G. Giacomelli[2], V. Gibson[5], W.R. Gibson[13], J.D. Gillies[20], J. Goldberg[22], M.J. Goodrick[5], W. Gorn[4], C. Grandi[2], F.C. Grant[5], J. Hagemann[27], G.G. Hanson[12], M. Hansroul[8], C.K. Hargrove[7], P.F. Harrison[13], J. Hart[8], P.M. Hattersley[1], M. Hauschild[8], C.M. Hawkes[8], E. Heflin[4], R.J. Hemingway[6], R.D. Heuer[8], J.C. Hill[5], S.J. Hillier[1], D.A. Hinshaw[18], J.D. Hobbs[8], P.R. Hobson[25], D. Hochman[26], R.J. Homer[1], A.K. Honma[28,a], S.R. Hou[17], C.P. Howarth[15], R.E. Hughes-Jones[16], R. Humbert[10], P. Igo-Kemenes[11], H. Ihssen[11], D.C. Imrie[25], A.C. Janissen[6], A. Jawahery[17], P.W. Jeffreys[20], H. Jeremie[18], M. Jimack[2], M. Jobes[1], R.W.L. Jones[13], P. Jovanovic[1], D. Karlen[6], K. Kawagoe[24], T. Kawamoto[24], R.K. Keeler[28], R.G. Kellogg[17], B.W. Kennedy[15], D.E. Klem[7], T. Kobayashi[24], T.P. Kokott[3], S. Komamiya[24], L. Köpke[8], J.F. Kral[8], R. Kowalewski[6], J. von Krogh[11], J. Kroll[9], M. Kuwano[24], P. Kyberd[13], G.D. Lafferty[16], F. Lamarche[18], J.G. Layter[4], P. Le Du[21], P. Leblanc[18], A.M. Lee[17], M.H. Lehto[15], D. Lellouch[26], P. Lennert[11], C. Leroy[18], J. Letts[4], S. Levegrün[3], L. Levinson[26], S.L. Lloyd[13], F.K. Loebinger[16], J.M. Lorah[17], B. Lorazo[18], M.J. Losty[7], X.C. Lou[12], J. Ludwig[10], M. Mannelli[8], S. Marcellini[2], G. Maringer[3], A.J. Martin[13], J.P. Martin[18], T. Mashimo[24], P. Mättig[3], U. Maur[3], J. McKenna[28], T.J. McMahon[1], J.R. McNutt[25], F. Meijers[8], D. Menszner[11], F.S. Merritt[9], H. Mes[7], A. Michelini[8], R.P. Middleton[20], G. Mikenberg[26], J. Mildenberger[6], D.J. Miller[15], C. Milstene[2,i], R. Mir[12], W. Mohr[10], C. Moisan[18], A. Montanari[2], T. Mori[24], T. Mouthuy[12,c], B. Nellen[3], H.H. Nguyen[9], S.W. O'Neale[8,d], F.G. Oakham[7], F. Odorici[2], M. Ogg[6], H.O. Ogren[12], H. Oh[4], C.J. Oram[28,a], M.J. Oreglia[9], S. Orito[24], J.P. Pansart[21], B. Panzer-Steindel[8], P. Paschievici[26], G.N. Patrick[20], N. Paz-Jaoshvili[23], P. Pfister[10], J.E. Pilcher[9], D. Pitman[28], D.E. Plane[8], P. Poffenberger[28], B. Poli[2], A. Pouladdej[6], E. Prebys[8], T.W. Pritchard[13], H. Przysiezniak[18], G. Quast[27], M.W. Redmond[9], D.L. Rees[1], G.E. Richards[16], K. Riles[4], S.A. Robins[13], D. Robinson[8], A. Rollnik[3], J.M. Roney[9], E. Ros[8], S. Rossberg[10], A.M. Rossi[2,e], M. Rosvick[28], P. Routenburg[6], K. Runge[10], O. Runolfsson[8], D.R. Rust[12], S. Sanghera[6], M. Sasaki[24], C. Sbarra[8], A.D. Schaile[10], O. Schaile[10], W. Schappert[6], P. Scharff-Hansen[8], P. Schenk[28], H. von der Schmitt[11], S. Schreiber[3], C. Schwick[27], J. Schwiening[3], W.G. Scott[20], M. Settles[12], B.C. Shen[4], P. Sherwood[15], R. Shypit[29], A. Simon[3], P. Singh[13], G.P. Siroli[2], A. Skuja[17], A.M. Smith[8], T.J. Smith[8], G.A. Snow[17], R. Sobie[28,f], R.W. Springer[17], M. Sproston[20], K. Stephens[16], J. Steuerer[28], R. Ströhmer[11], D. Strom[9,g], H. Takeda[24], T. Takeshita[24,h], P. Taras[18], S. Tarem[26], P. Teixeira-Dias[11], N. Tesch[3], N.J. Thackray[1], G. Transtromer[25], N.J. Tresilian[16], T. Tsukamoto[24], M.F. Turner[5], G. Tysarczyk-Niemeyer[11], D. Van den plas[18], R. Van Kooten[8],

G.J. VanDalen[4], G. Vasseur[21], C.J. Virtue[7], A. Wagner[27], D.L. Wagner[9], C. Wahl[10], J.P. Walker[1], C.P. Ward[5], D.R. Ward[5], P.M. Watkins[1], A.T. Watson[1], N.K. Watson[8], M. Weber[11], P. Weber[6], S. Weisz[8], P.S. Wells[8], N. Wermes[11], M.A. Whalley[1], G.W. Wilson[21], J.A. Wilson[1], V-H. Winterer[10], T. Wlodek[26], S. Wotton[11], T.R. Wyatt[16], R. Yaari[26], G. Yekutieli[26], M. Yurko[18], W. Zeuner[8], G.T. Zorn[17].

[1]School of Physics and Space Research, University of Birmingham, Birmingham, B15 2TT, UK
[2]Dipartimento di Fisica dell' Università di Bologna and INFN, Bologna, 40126, Italy
[3]Physikalisches Institut, Universität Bonn, D-5300 Bonn 1, FRG
[4]Department of Physics, University of California, Riverside, CA 92521 USA
[5]Cavendish Laboratory, Cambridge, CB3 0HE, UK
[6]Carleton University, Dept of Physics, Colonel By Drive, Ottawa, Ontario K1S 5B6, Canada
[7]Centre for Research in Particle Physics, Carleton University, Ottawa, Ontario K1S 5B6, Canada
[8]CERN, European Organisation for Particle Physics, 1211 Geneva 23, Switzerland
[9]Enrico Fermi Institute and Department of Physics, University of Chicago, Chicago Illinois 60637, USA
[10]Fakultät für Physik, Albert Ludwigs Universität, D-7800 Freiburg, FRG
[11]Physikalisches Institut, Universität Heidelberg, Heidelberg, FRG
[12]Indiana University, Dept of Physics, Swain Hall West 117, Bloomington, Indiana 47405, USA
[13]Queen Mary and Westfield College, University of London, London, E1 4NS, UK
[14]Birkbeck College, London, WC1E 7HV, UK
[15]University College London, London, WC1E 6BT, UK
[16]Department of Physics, Schuster Laboratory, The University, Manchester, M13 9PL, UK
[17]Department of Physics and Astronomy, University of Maryland, College Park, Maryland 20742, USA
[18]Laboratoire de Physique Nucléaire, Université de Montréal, Montréal, Quebec, H3C 3J7, Canada
[20]Rutherford Appleton Laboratory, Chilton, Didcot, Oxfordshire, OX11 0QX, UK
[21]DPhPE, CEN Saclay, F-91191 Gif-sur-Yvette, France
[22]Department of Physics, Technion-Israel Institute of Technology, Haifa 32000, Israel
[23]Department of Physics and Astronomy, Tel Aviv University, Tel Aviv 69978, Israel
[24]International Centre for Elementary Particle Physics and Dept of Physics, University of Tokyo, Tokyo 113, and Kobe University, Kobe 657, Japan
[25]Brunel University, Uxbridge, Middlesex, UB8 3PH UK
[26]Nuclear Physics Department, Weizmann Institute of Science, Rehovot, 76100, Israel
[27]Universität Hamburg/DESY, II Inst für Experimental Physik, 2000 Hamburg 52, Germany
[28]University of Victoria, Dept of Physics, P O Box 3055, Victoria BC V8W 3P6, Canada
[29]University of British Columbia, Dept of Physics, 6224 Agriculture Road, Vancouver BC V6T 1Z1, Canada

[a]Also at TRIUMF, Vancouver, Canada V6T 2A3
[b]Now at Meiji Gakuin University, Yokohama 244, Japan
[c]Now at Centre de Physique des Particules de Marseille, Faculté des Sciences de Luminy, Marseille

[d]On leave from Birmingham University, Birmingham B15 2TT, UK
[e]Now at Dipartimento di Fisica, Università della Calabria and INFN, 87036 Rende, Italy
[f]And IPP, McGill University, High Energy Physics Department, 3600 University Str, Montreal, Quebec H3A 2T8, Canada
[g]Now at Dept of Physics, University of Oregon, Eugene, Oregon 97405
[h]Also at Shinshu University, Matsumoto 390, Japan
[i]Now at Tel Aviv University, Israel.

1 Introduction

This letter reports on the measurement of the inclusive branching ratios of the τ lepton to final states containing one, three and five charged particles (1, 3 and 5-prong decays). It is based on a high statistics sample of $e^+e^- \to \tau^+\tau^-$ events collected using the OPAL detector, at centre-of-mass energies between 88.2 and 94.2 GeV, during the 1990 and 1991 LEP running periods. At these energies it is possible to obtain an extremely clean sample of τ decays with minimal bias against any particular decay mode. This, combined with the good tracking and particle identification capabilities of the OPAL detector, makes possible a precise measurement of the topological branching ratios of the τ lepton.

The main interest in this measurement stems from the so-called "missing decay mode" problem. Previous measurements of τ decays [1] suggest an inconsistency between the inclusive 1-prong branching ratio (86.1±0.3%) and the sum of the 1-prong exclusive branching ratios ($< 80.2 \pm 1.4\%$ where theoretical constraints are used to limit poorly measured channels) [2, 3]. This discrepancy is not resolved by including recent measurements of the topological branching ratios [4, 5, 6]. There are also discrepancies between the measurements of the inclusive branching ratios. For example, the HRS collaboration measures an inclusive 1-prong branching ratio of 86.4±0.3±0.3% [7] while the CELLO collaboration reports a value of 84.9±0.4±0.3% [8].

2 The OPAL detector

The OPAL detector is a large general-purpose detector covering almost the entire solid angle [9]. A coordinate system is defined such that the z axis is along the e^- beam direction and θ is the polar angle. Central tracking chambers, located in a 0.435 T solenoidal magnetic field, measure the momenta of charged particles. The central detector consists of three sets of drift chambers: a high precision vertex chamber, a large-volume jet chamber and "z-chambers" which give a precise z measurement in the barrel region. The jet chamber is divided into 24 azimuthal sectors each containing 159 sense wires. The measurement of the charge deposition in the jet chamber provides particle identification using dE/dx information. A barrel time-of-flight (TOF) counter array surrounds the coil in the region $|\cos\theta| < 0.82$, which is in turn surrounded by an electromagnetic calorimeter (ECAL) with a presampler. The ECAL consists of a barrel part, covering the region $|\cos\theta| < 0.82$, which contains 9440 lead-glass blocks pointing towards the interaction region, and two endcaps covering the region $0.81 < |\cos\theta| < 0.98$, consisting of 2264 lead-glass blocks parallel to the beam direction. The amount of material in front of the ECAL in the region $|\cos\theta| < 0.7$ is approximately $2X_0/\sin\theta$ (where X_0 is one radiation length). The magnet return yoke is instrumented with nine layers of streamer tubes which serve as a hadron calorimeter (HCAL) and muon tracker. On the outside of the detector four layers of (MUON) drift chambers are used for muon detection. The luminosity is measured using small-angle Bhabha scattering with two forward detector calorimeters between 40 and 120 mrad from the beam direction.

Between the end of the 1990 run and the start of the 1991 run the original (7.8 cm radius) beam pipe was removed and a new beam pipe and silicon microvertex detector were installed inside the existing vertex chamber. While the microvertex detector is not used in this anal-

ysis it did introduce some additional material. This leads to an increased number of photon conversions within the central detector in the 1991 data, compared to the 1990 data sample.

The momentum resolution of the tracking chambers is measured to be $\Delta p/p \approx 6.8\%$ for $p_\perp = 45$ GeV from $e^+e^- \to \mu^+\mu^-$ events, where $p_\perp$ is the momentum transverse to the beam. In the barrel region the ECAL gives an energy resolution of $\Delta E/E \approx 3\%$ for $E \approx 45$ GeV from $e^+e^- \to e^+e^-$ events. The optimum dE/dx performance of the jet chamber is $\sigma_{dE/dx} = 0.030(dE/dx)$ if 159 points are measured on an isolated track. For Monte Carlo studies the OPAL detector response is simulated by a program [10] which treats in detail the detector geometry and material as well as effects of detector resolutions and efficiencies.

3 Selection of $e^+e^- \to \tau^+\tau^-$ events

The procedure used to select τ pair events is very similar to that described in previous OPAL publications [11, 12]. The distinctive signature of a τ pair event is two almost back-to-back jets of one or more charged particles, often accompanied by neutral hadrons or photons. Each jet is accompanied by "missing energy" from the production of one or more neutrinos.

There are four main backgrounds to consider. The first two are $e^+e^- \to e^+e^-$ and $e^+e^- \to \mu^+\mu^-$ events, which can be identified by the presence of two very high-momentum, back-to-back charged particles with the full centre-of-mass energy, $E_{\rm CM}$, deposited in the electromagnetic calorimeter for $e^+e^- \to e^+e^-$ and with very little ECAL energy for $e^+e^- \to \mu^+\mu^-$. Hermeticity of the calorimeter ensures correct identification of $e^+e^- \to e^+e^-\gamma$ and $e^+e^- \to \mu^+\mu^-\gamma$ events which have been a troublesome background for some previous experiments. A third background to $e^+e^- \to \tau^+\tau^-$ events comes from $e^+e^- \to q\bar{q}$ (multihadronic) events. This background is less significant at LEP than at lower-energy experiments because the particle multiplicity in $e^+e^- \to q\bar{q}$ events increases with $E_{\rm CM}$, while for τ decays it remains constant. Finally, a fourth background comes from two-photon processes $e^+e^- \to (e^+e^-)X$ where the final-state electron and positron escape undetected at low angles and the system X is misidentified as a low-visible-energy τ pair event. The contribution to the background from these processes is small because they lack the enhancement to the cross-section from the Z^0 resonance and because the visible energy of the two-photon system is in general much smaller than that from a τ pair event.

Other potential backgrounds arising from cosmic rays and single-beam interactions can be suppressed with straightforward requirements on TOF, on the location of the primary event vertex and on event topology. The consequence of the naturally reduced backgrounds to $e^+e^- \to \tau^+\tau^-$ at LEP is that high purity can be attained without sacrificing selection efficiency or strongly biasing for or against certain τ decay modes. This substantially reduces the systematic uncertainties in the branching ratio measurements introduced by the event selection.

In selecting τ pair events only "good" charged tracks and electromagnetic clusters are considered. In this analysis, a good charged track must have $p_\perp > 100$ MeV, a measured $|d_0|<2$ cm, and a measured $|z_0|<75$ cm, where $|d_0|$ is the distance of closest approach of the track to the beam axis, and $|z_0|$ is the displacement along the beam axis from the nominal interaction point at the point of closest approach to the beam. The track must also have at least 20 measured space points (hits) in the jet chamber. In the barrel, a good ECAL cluster, which is a group

of one or more contiguous lead-glass blocks, must have a minimum energy of 100 MeV. In the endcap, the minimum cluster energy is 200 MeV, and the shower cluster must contain at least two lead-glass blocks, no one of which may contribute more than 99% to the cluster's energy.

So as to minimise the bias against 1-5 and 3-3 topology events[1] somewhat looser cuts are used to eliminate multihadrons than in the general τ pair selection. The number of good charged tracks must be in the range from two to eight and the sum of the number of good charged tracks and the number of good ECAL clusters must be less than 18. The cosmic ray background is removed by requiring that there be at least one good charged track with a measured $|d_0| < 0.5$ cm and a measured $|z_0| < 20$ cm and requiring that the magnitude of the average z_0 of all good tracks be less than 20 cm. In addition, the TOF must give a signal consistent with that of an event originating from an e^+e^- collision.

For this analysis, it is convenient to treat each τ decay as a jet, as defined in ref. [11], where charged tracks and ECAL clusters are assigned to cones of half-angle 35°. A τ pair candidate must contain exactly two jets, each with at least one charged track and with a total track and cluster energy exceeding 1% of the beam energy. To remove backgrounds from two-photon processes and to remove events with energetic photon radiation, the acolinearity between the two jets must be less than 15°, where the directions of the jets are given by the vector sums of the momenta of the tracks and clusters. The events are restricted to the barrel region of the detector by requiring that the average value of $|\cos\theta|$ for the two jets satisfy $\overline{|\cos\theta|} < 0.7$. This cut is applied in order to eliminate systematic biases introduced by the more severe requirements necessary to reject the $e^+e^- \to e^+e^-$ background in the overlap region of the barrel and endcap components of the electromagnetic calorimeter.

Background from $e^+e^- \to e^+e^-$ events is eliminated by requirements on the total ECAL energy and the weighted charged track and ECAL energy as for previous OPAL analyses [12]. Events are identified as $e^+e^- \to \mu^+\mu^-$ events by the muon pair selection described in ref. [11]; a track in each hemisphere must give a signal consistent with that for a muon in any two out of the ECAL, HCAL or MUON subdetectors and the scalar sum of the charged track momenta plus the energy of the most energetic ECAL cluster must be greater than $0.6E_{\rm CM}$. Most of the residual background from $e^+e^- \to (e^+e^-)X$ events is rejected by requirements on the total visible energy and the missing transverse momenta as described in ref. [12].

These selection criteria were applied to all the data collected during 1990 and 1991, where the detector components important to the analysis were fully operational, to give a sample of 3794 τ pair candidate events for the 1990 run and 8913 events for the 1991 run. The data were collected at centre-of-mass energies between 88.2 and 94.2 GeV, with approximately 75% collected on the peak of the Z^0 resonance. From Monte Carlo studies [13] the selection efficiency was estimated to be 57.1±0.2%. This corresponds to an efficiency of 92.0% within the $|\cos\theta| < 0.7$ angular acceptance. The bias introduced by the event selection cuts is given in table 1, the errors on these bias factors are dominated by Monte Carlo statistics. The efficiency for selecting events with a 1-3 topology is slightly greater than that for events with a 1-1 topology because of the cuts necessary to eliminate $e^+e^- \to e^+e^-$ and $e^+e^- \to \mu^+\mu^-$ events. Within the Monte Carlo statistical errors there is no significant bias against events with a 3-3 or 1-5 topology.

[1] An event with i charged tracks in one hemisphere and j charged tracks in the opposite hemisphere is referred to as having an i-j topology.

Event topology	Bias factor
1-1	0.995±0.001
1-3	1.015±0.004
3-3	0.997±0.016
1-5	0.964±0.048

Table 1: The acceptance for the different τ pair event topologies relative to the overall τ pair acceptance.

Background	Contamination(%)
$e^+e^- \to q\bar{q}$	1.0±0.3
$e^+e^- \to e^+e^-$	0.3±0.3
$e^+e^- \to \mu^+\mu^-$	0.5±0.5
$e^+e^- \to (e^+e^-)X$	0.1±0.1
Total	1.9±0.7

Table 2: Estimated background contaminations in the 12707 τ pair candidate events. The errors include both statistical and systematic uncertainties.

Monte Carlo studies of $e^+e^- \to e^+e^-$ [14], $e^+e^- \to \mu^+\mu^-$ [13], $e^+e^- \to q\bar{q}$ [15] and $e^+e^- \to (e^+e^-)X$ [16] events give the residual backgrounds shown in table 2. The total background is found to be 1.9±0.7% of the total number of events. The main contribution to the systematic uncertainty on the background to events with a 1-1 topology is from muon pair events which are not eliminated by the total energy requirement. The size of this effect is estimated from detailed comparisons of muon pair events with Monte Carlo. For events with topologies other than 1-1 the background is predominantly from multihadrons. In this case an overall systematic uncertainty is obtained by using an algorithm which tags candidate τ pair events using only one hemisphere of the event, for events which are identified as multihadrons from the properties of the opposite hemisphere. Assuming that the two hemispheres of the event correspond to two jets which fragment independently, a comparison of the background estimates from the data and the Monte Carlo is used to derive a systematic uncertainty of ±25% on the background from multihadrons.

The 11262 events for which the forward detector was fully operational correspond to a total integrated luminosity of 17.4 pb^{-1}. From the estimated acceptance and the measured integrated luminosity [11] and standard model τ pair cross-section at each energy point [13], totals of 3730 τ pair events for the 1990 run and 7307 τ pair events for the 1991 run are predicted. These predictions are in good agreement with the measured numbers of events after background subtraction (3712 events for the 1990 run and 7336 events for the 1991 run).

4 Measurement of the τ branching ratios

In this analysis the τ topological branching ratios are measured using an unfolding technique. The migration of events from one topology to another caused by tracking inefficiencies, photon conversions and K^0_S decays are taken into account using the Monte Carlo simulation of the detector [10]. The inclusive 1, 3 and 5-prong branching ratios are determined from a simultaneous fit to the numbers of events with each measured topology. The additional requirements used to minimise the effects of tracking inefficiencies and the method used to identify tracks originating from photon conversions are described below.

4.1 Track reconstruction effects

Tracks may either be lost or split because of the effects of the track reconstruction. In particular, tracks may be lost in 3-prong or 5-prong τ decays where two of the particles are produced with trajectories which overlap within the two hit resolution of the jet chamber, or tracks may be split close to the anode and cathode planes of the jet chamber.

The measured number of jet chamber hits per track for 1, 2, 3 and >3-prong decays is compared with the Monte Carlo prediction in figure 1. For a straight, isolated track, in the barrel region of the detector, a maximum of 159 points can be measured. For jets with more than one associated track the measured number of hits per track may be reduced where two tracks overlap, this effect is well described by the Monte Carlo. For jets with only one associated track, a small excess in the number of tracks with less than 50 hits in the data over the Monte Carlo prediction is visible. Detailed studies show that this effect corresponds to additional split tracks in the data, where part of the track is lost and so the measured number of hits is reduced. Most of these split tracks occur close to the anode and cathode planes of the jet chamber.

For the multiplicity measurement, good charged tracks must have at least 50 jet chamber hits and a momentum greater than 250 MeV (to ensure good electron identification using dE/dx). In $0.14\pm0.03\%$ of the τ candidates all the charged tracks associated to the jet are eliminated by these cuts (compared to the Monte Carlo prediction of $0.09\pm0.01\%$), in this case the multiplicity is assigned to be one.

4.2 Identification of photon conversions

Secondary tracks are produced in the detector from photon conversions and hadronic interactions. Approximately 80% of these are electrons or positrons from photon conversions, where the photons are produced from electromagnetic π^0 decays. Secondary electrons are identified using either the dE/dx measurement alone (which gives a high electron identification efficiency at low momenta, but a reduced efficiency for high momentum electrons because of the poorer $e-\pi$ separation at high momenta) or a selection which combines looser dE/dx requirements with the reconstruction of secondary vertices in the central detector (which has an efficiency which is relatively independent of momentum).

The dE/dx based electron identification uses the difference between the measured dE/dx and the expected dE/dx for a pion, $(dE/dx)^{\pi}$, normalised to the error on the dE/dx measurement, $\sigma_{dE/dx}$:

$$\Delta E^{\pi} = \frac{dE/dx - (dE/dx)^{\pi}}{\sigma_{dE/dx}}.$$

The quantity $(dE/dx)^{\pi}$ is obtained from a parameterization of the dE/dx distribution as a function of momentum in the τ pair data from tracks which are classified as either electrons, muons or pions using criteria similar to those used in the exclusive branching ratio measurement [12] and which are independent of the dE/dx measurement. This parameterization is also used for the dE/dx simulation in the Monte Carlo. In addition to the track quality cuts described above, for the dE/dx measurement to be used, the number of samples, $n_h^{dE/dx}$, must satisfy $n_h^{dE/dx} \geq 20$. The dE/dx resolution is measured to be

$$\sigma_{dE/dx} = \sigma_{min} \left(\frac{159}{n_h^{dE/dx}} \right)^{0.43} \left(\frac{dE}{dx} \right)$$

where $\sigma_{min} = 0.033$ for the 1990 data and $\sigma_{min} = 0.034$ for the 1991 data. ΔE^{π} is plotted in different momentum regions in figure 2. A track is classified as an electron if $\Delta E^{\pi} > 2.5$.

The second means of identifying photon conversions considers all pairs of oppositely charged tracks, both with $\Delta E^{e} > -2$, where

$$\Delta E^{e} = \frac{dE/dx - (dE/dx)^{e}}{\sigma_{dE/dx}}$$

and $(dE/dx)^{e}$ is the expected dE/dx for an electron. At the point of closest approach in the xy plane, where the tangents of the two tracks are parallel, the tracks must have a separation of less than 0.3 cm in xy and 50 cm in z, the cosine of the opening angle between the two tracks must be greater than 0.99 and the cosine of the angle between the vector sum of the momenta of the tracks and the position vector from the origin to the secondary vertex must be greater than 0.996. In addition, the distance from the beam axis to the secondary vertex, r_{conv}, must satisfy $3 < r_{conv} < 200$ cm, the distance from the beam axis to the first hit on either track must be greater than $r_{conv} - 20$ cm and the reconstructed photon invariant mass must be less than 0.2 GeV. The radial distribution of identified conversions in data and Monte Carlo for both the 1990 and 1991 detector configurations are shown in figure 3. The excess in the data compared to the Monte Carlo prediction at $r_{conv} = 25$ cm is caused by material known to be missing from the Monte Carlo simulation used for this analysis.

The efficiency for rejecting conversion electrons and the loss of incorrectly identified pions, as estimated from the Monte Carlo are given in table 3. By identifying electrons using either of the two criteria it is possible to obtain an overall efficiency of order 90% with a minimal loss of pion tracks from 3-prong or 5-prong τ decays.

A control sample of 781 visually scanned $e^+e^- \to e^+e^-\gamma$ and $e^+e^- \to \mu^+\mu^-\gamma$ events, where the radiated photon converts within the central detector to give an e^+e^- pair, provides an independent check on the efficiency for tagging photon conversions. The measured efficiency is compared with the Monte Carlo prediction in table 4. Combining the efficiency from events with one additional track with that from events with two additional tracks, both of which are

	conversion electron identification efficiency(%)	pion misidentification probability(%)
dE/dx cuts	82±1	0.23±0.01
vertex cuts	67±1	0.23±0.01
dE/dx or vertex cuts	89±1	0.46±0.02

Table 3: The efficiency for identifying electrons from photon conversions and loss of pions from τ decays using criteria based on either dE/dx alone, geometrical cuts based on reconstructing secondary vertices or either of the two selections, as estimated from Monte Carlo.

	number of conversion tracks	conversion finding efficiency (%)			
		(a) dE/dx cuts	(b) vertex cuts	(a) or (b)	
data	1	86±5	53±4	89±5	} 76±3
	2	55±4	60±4	70±4	
Monte Carlo	1	77±4	53±3	82±4	} 81±3
	2	64±3	73±4	81±4	

Table 4: Comparison of the efficiency for identifying conversion electrons using a control sample of $e^+e^- \to e^+e^-\gamma \to e^+e^-e^+e^-$ and $e^+e^- \to \mu^+\mu^-\gamma \to \mu^+\mu^-e^+e^-$ events, with predictions from Monte Carlo.

identified as electrons, where these contributions are weighted as in τ pair events, gives a discrepancy between data and Monte Carlo of 5±4%. From this a conservative overall systematic uncertainty of ±10% is assigned to the efficiency for identifying conversion electrons.

The corrected track multiplicity is obtained by subtracting the number of identified electrons from the number of "good" tracks associated to each jet. Since genuine primary electrons may be produced from $\tau \to e\nu\bar{\nu}$ decays and in order to minimise the efficiency loss for 3 or 5-prong decays where one pion is incorrectly identified as an electron, the corrected track multiplicity is increased by one if the result after subtraction is an even number (assuming one or more electrons have been found). Since the probability of misidentifying two pions as electrons is small, this is not a significant source of systematic uncertainty on the branching ratio measurement.

4.3 Unfolding the topological branching ratios

The τ lepton must decay to an odd number of charged particles, where the branching ratios to higher charged multiplicities are heavily suppressed; the 5-prong branching ratio is of order 0.1%, while the upper limit on the 7-prong branching ratio is $B_7 < 0.019\%$ [1]. In practice, however, the measured charged track multiplicity distribution is distorted by errors in the track reconstruction and by secondary tracks produced in the detector from photon conversions and hadronic interactions. To unfold the "true" number of τ decays to 1, 3 and 5-prongs, efficiencies and cross-contaminations between the different event topologies obtained from Monte Carlo simulation are used. Four possible true event topologies are considered here: 1-1, 1-3, 3-3 and

	1990 data			1991 data		
$i-j$	n_{ij}	n_{ij}^B	n_{ij}^{fit}	n_{ij}	n_{ij}^B	n_{ij}^{fit}
$1-1$	2663	34.2 ± 22.8	$2618.3 \pm 19.2 \pm 7.4$	6094	80.2 ± 53.5	$5994.9 \pm 30.5 \pm 23.9$
$1-2$	65	1.0 ± 0.7	$55.8 \pm 2.8 \pm 9.2$	144	2.3 ± 1.6	$166.3 \pm 5.2 \pm 28.2$
$1-3$	901	1.5 ± 0.9	$927.5 \pm 11.4 \pm 10.7$	2247	3.5 ± 2.0	$2248.3 \pm 19.6 \pm 34.3$
$1-4$	12	4.4 ± 1.5	$8.5 \pm 1.2 \pm 1.0$	41	10.4 ± 3.5	$28.4 \pm 2.3 \pm 3.4$
$1-5$	22	3.5 ± 1.3	$18.2 \pm 2.0 \pm 1.1$	66	8.1 ± 3.1	$58.3 \pm 3.7 \pm 3.8$
$2-2$	2	2.5 ± 1.1	$0.1 \pm 0.1 \pm 0.0$	3	5.8 ± 2.6	$0.7 \pm 0.3 \pm 0.0$
$2-3$	19	2.0 ± 1.0	$8.4 \pm 1.1 \pm 1.2$	36	4.6 ± 2.3	$28.8 \pm 2.3 \pm 4.9$
$3-3$	98	5.9 ± 1.7	$81.7 \pm 3.3 \pm 1.6$	223	13.9 ± 4.0	$204.8 \pm 6.1 \pm 5.7$
Total	3782	54.8 ± 23.0	$3718.4 \pm 22.9 \pm 16.1$	8854	128.8 ± 54.0	$8730.5 \pm 37.4 \pm 51.2$

Table 5: The measured number of events with each topology, n_{ij}, the estimated distribution for the background, n_{ij}^B, and the predicted number of events in each topology from the Monte Carlo using the fitted branching ratios, $n_{ij}^{fit} = \sum_{kl} \epsilon_{kl \to ij} f_{kl} N_{kl}$.

1-5. The corrected number of events in each class, N_{kl}, is related to the measured number of events with an i-j topology, n_{ij}, by

$$n_{ij} - n_{ij}^B = \sum_{kl} \epsilon_{kl \to ij} f_{kl} N_{kl}$$

where n_{ij}^B is the estimated non-τ background, f_{kl} is the bias introduced by the event selection and $\epsilon_{kl \to ij}$ is the probability of a τ pair event with a "true" k-l topology resulting in a measured i-j topology. The inclusive branching ratios, B_1, B_3 and B_5, are then given by

$$N_{kl} = (2 - \delta_{kl}) B_k B_l N_{tot}$$

where N_{tot} is the total number of τ pair events. The branching ratios are obtained from a simultaneous fit to the numbers of events with the topologies listed in table 5. Of the 71 events eliminated by restricting the fit to these topologies ≈ 58 correspond to background from $e^+e^- \to q\bar{q}$ events. This method has the advantage that it is independent of the integrated luminosity measurement and the overall efficiency of the τ pair selection and so gives a smaller systematic error on the branching ratio measurement than if the absolute number of events in each topology were used.

The ϵ matrix which describes the efficiency and cross-contamination between decay modes is given in table 6. The additional material introduced with the microvertex detector necessitates treating the 1990 and 1991 data separately. The most important contributions to the off-diagonal elements of the ϵ matrix are from the track reconstruction and from secondary tracks produced in the detector, as described below:

- The merging of overlapping tracks is the dominant contribution to $\epsilon_{13 \to 11}$, $\epsilon_{13 \to 12}$, $\epsilon_{15 \to 13}$, $\epsilon_{15 \to 14}$, $\epsilon_{33 \to 13}$ and $\epsilon_{33 \to 23}$. Comparing the number of events with a 1-2 topology between data and Monte Carlo (over 60% of which have a "true" 1-3 topology) reveals an excess of $17 \pm 9\%$ in the Monte Carlo. From this a conservative systematic error of $\pm 25\%$ is assigned to these elements of the ϵ matrix.

$\epsilon_{kl\to ij}(\%)$	1990 detector			
ij	$kl = 1{-}1$	$kl = 1{-}3$	$kl = 1{-}5$	$kl = 3{-}3$
$1{-}1$	$97.72 \pm 0.72 \pm 0.27$	$0.31 \pm 0.07 \pm 0.08$	< 1.9	< 0.2
$1{-}2$	$0.83 \pm 0.07 \pm 0.14$	$3.53 \pm 0.23 \pm 0.88$	< 1.9	< 0.2
$1{-}3$	$1.39 \pm 0.09 \pm 0.24$	$93.61 \pm 1.18 \pm 0.91$	$5.7 \pm 3.3 \pm 1.4$	$0.3 \pm 0.2 \pm 0.1$
$1{-}4$	< 0.1	$0.58 \pm 0.09 \pm 0.09$	$17.1 \pm 5.7 \pm 4.3$	< 0.2
$1{-}5$	< 0.1	$0.63 \pm 0.10 \pm 0.09$	$76.9 \pm 12.1 \pm 4.5$	< 0.2
$2{-}2$	< 0.1	< 0.1	< 1.9	< 0.2
$2{-}3$	< 0.1	$0.41 \pm 0.08 \pm 0.06$	< 1.9	$5.2 \pm 0.9 \pm 1.3$
$3{-}3$	< 0.1	$0.81 \pm 0.11 \pm 0.12$	< 1.9	$92.4 \pm 4.0 \pm 1.3$
$\epsilon_{kl\to ij}(\%)$	1991 detector			
ij	$kl = 1{-}1$	$kl = 1{-}3$	$kl = 1{-}5$	$kl = 3{-}3$
$1{-}1$	$96.82 \pm 0.49 \pm 0.38$	$0.38 \pm 0.05 \pm 0.10$	< 0.8	< 0.1
$1{-}2$	$1.00 \pm 0.05 \pm 0.17$	$4.52 \pm 0.18 \pm 1.13$	< 0.8	< 0.1
$1{-}3$	$2.03 \pm 0.07 \pm 0.34$	$91.68 \pm 0.82 \pm 1.16$	$2.3 \pm 1.4 \pm 0.6$	$1.0 \pm 0.3 \pm 0.2$
$1{-}4$	< 0.1	$0.89 \pm 0.08 \pm 0.13$	$14.1 \pm 3.3 \pm 3.5$	< 0.1
$1{-}5$	< 0.1	$1.04 \pm 0.09 \pm 0.16$	$82.0 \pm 8.0 \pm 3.6$	< 0.1
$2{-}2$	< 0.1	< 0.1	< 0.8	< 0.1
$2{-}3$	< 0.1	$0.41 \pm 0.06 \pm 0.06$	< 0.8	$8.9 \pm 0.9 \pm 2.2$
$3{-}3$	< 0.1	$0.92 \pm 0.08 \pm 0.14$	< 0.8	$87.1 \pm 2.8 \pm 2.2$

Table 6: The efficiency and cross-contamination between decay modes, $\epsilon_{kl\to ij}$, estimated from Monte Carlo studies for the 1990 and the 1991 detector configuration. The first error is from Monte Carlo statistics, while the second error is from systematic studies described in the text.

- Secondary tracks from photon conversions and hadronic interactions are the dominant contribution to $\epsilon_{11\to 12}$, $\epsilon_{11\to 13}$, $\epsilon_{13\to 23}$, $\epsilon_{13\to 33}$, $\epsilon_{13\to 14}$ and $\epsilon_{13\to 15}$. Three potential sources of systematic error on these quantities are considered. Firstly, the discrepancy shown in figure 3 was investigated by generating additional Monte Carlo events with a corrected material distribution and re-evaluating the ϵ matrix. This gives a systematic error on these quantities of $\pm 13\%$. Secondly, the effect of the systematic error on the efficiency for identifying photon conversions was estimated by varying the conversion finding efficiency in the Monte Carlo by $\pm 10\%$. This leads to an additional $\pm 7\%$ systematic uncertainty on these elements of the ϵ matrix. Finally, if the number of π^0s per τ decay is not correctly modelled by the Monte Carlo this may bias the result. The main source of uncertainty is the relatively poorly measured $\tau \to \pi^{\pm} 3\pi^0 \nu$ branching fraction. Varying this between 0 and 5% gives an additional systematic error of $\pm 9\%$ on $\epsilon_{11\to 12}$ and $\epsilon_{11\to 13}$.

- There is also a contribution to $\epsilon_{11\to 12}$ and $\epsilon_{11\to 13}$ from $\tau \to \mathrm{K}^*\nu$ decays, where the K^* decays via a K^0_S which subsequently decays as $\mathrm{K}^0_\mathrm{S} \to \pi^+\pi^-$. Since the branching ratio for this process is small ($\sim$0.5%) this does not contribute significantly to the systematic error.

The measured number of events and the expected non-τ background for each topology are given in table 5. The backgrounds from $\mathrm{e^+e^-} \to \mathrm{e^+e^-}$, $\mathrm{e^+e^-} \to \mu^+\mu^-$ and $\mathrm{e^+e^-} \to (\mathrm{e^+e^-})X$ events nearly all have a 1-1 topology, while the multiplicity distribution for the multihadronic

	$\Delta B_1(\%)$	$\Delta B_3(\%)$	$\Delta B_5(\%)$
non-τ background	± 0.14	± 0.13	± 0.035
track reconstruction	± 0.12	± 0.12	± 0.012
γ conversions	± 0.10	± 0.10	± 0.027
event selection	± 0.10	± 0.10	–
Total	± 0.23	± 0.22	± 0.046

Table 7: Systematic errors on the measurement of B_1, B_3 and B_5 as a fraction of the total number of τ decays, for the combined measurement from both 1990 and 1991 data.

background is taken from the Monte Carlo prediction. The error on the $e^+e^- \to e^+e^-$, $e^+e^- \to \mu^+\mu^-$ and $e^+e^- \to (e^+e^-)X$ backgrounds includes both Monte Carlo statistical and systematic errors. The error on the multihadron background is from Monte Carlo statistics only, the overall systematic scale uncertainty is considered below.

A χ^2 fit to the 1990 data with $B_1 + B_3 + B_5$ constrained to equal one and with any two out of B_1, B_3 and B_5 as free parameters, gives $B_1 = 85.10 \pm 0.48 \pm 0.17\%$, $B_3 = 14.67 \pm 0.47 \pm 0.16\%$ and $B_5 = 0.23 \pm 0.10 \pm 0.04\%$ with a χ^2 of 5.6 for five degrees of freedom. A fit to the 1991 data gives $B_1 = 84.22 \pm 0.32 \pm 0.20\%$, $B_3 = 15.51 \pm 0.32 \pm 0.20\%$ and $B_5 = 0.27 \pm 0.08 \pm 0.04\%$ with a χ^2 of 2.1 for five degrees of freedom. Here, the first error is the combined statistical error from the data and the τ pair Monte Carlo and the second error is from the error on the non-τ background and the systematic errors on the ϵ matrix. The Monte Carlo prediction for the number of events in each bin using the fitted branching ratios is given in table 5. The agreement between data and Monte Carlo is good.

There are two further sources of systematic error to be considered. Scaling the hadronic background by $\pm 25\%$ and re-applying the fit gives an estimate of the uncertainty introduced by the systematic error on the level of the multihadronic background. This gives a contribution to the systematic error on B_1, B_3 and B_5 (as a fraction of the total number of τ decays) of $\pm 0.07\%$, $\pm 0.05\%$ and $\pm 0.023\%$ respectively. The dominant source of systematic error from the event selection is from the cut on the mean jet $|\cos\theta|$ which is used to define the angular acceptance. Varying this cut between 0.65 and 0.75 and repeating the analysis gives an additional contribution to the systematic error on B_1 and B_3 of 0.1% of the number of τ decays. The cuts used to identify muon pair events were varied to estimate the effect on the branching ratio measurement of the systematic errors on the bias factors quoted in table 1. The contribution to the overall systematic error from this source is negligible.

The sources of systematic error on the measurement of B_1, B_3 and B_5 are summarised in table 7. Varying the number of jet chamber hits required for a "good" track between 30 and 80 and repeating the analysis provides an additional check on the systematic error introduced by the track reconstruction. This gives a variation in the fitted branching ratios consistent with the systematic error quoted in table 7.

5 Summary and discussion

The inclusive branching ratios of the τ lepton to one, three and five charged particle final states are measured to be $B_1 = 84.48 \pm 0.27(stat) \pm 0.23(sys)\%$, $B_3 = 15.26 \pm 0.26 \pm 0.22\%$ and $B_5 = 0.26 \pm 0.06 \pm 0.05\%$ respectively. These measurements have been obtained from a fit where $B_1 + B_3 + B_5$ is constrained to equal one. The correlations between the fitted branching ratios are given by the matrix

$$\rho = \begin{pmatrix} 1.0 & -0.97 & -0.15 \\ -0.97 & 1.0 & -0.07 \\ -0.15 & -0.07 & 1.0 \end{pmatrix}.$$

While the measurements of B_1 and B_3 are highly correlated, the measurement of B_5 is relatively independent of B_1 and B_3.

The measured 5-prong branching ratio is in agreement with the 1990 Particle Data Group world average [1]. However, the measured 1-prong branching ratio is lower than the world average by more than three standard deviations while the 3-prong branching fraction is correspondingly higher than the average value. This confirms the results obtained by the CELLO collaboration [8] which also gave a 1-prong branching ratio which was significantly smaller than previous measurements. It is also in agreement with the results obtained by other LEP experiments [4]. While this is not sufficient by itself to resolve the "missing decay mode" problem it does go some way towards reducing the size of the effect.

Acknowledgements

It is a pleasure to thank the SL Division for the efficient operation of the LEP accelerator, and for its continuing close cooperation with our experimental group. In addition to the support staff at our own institutions we are pleased to acknowledge the
Department of Energy, USA,
National Science Foundation, USA,
Science and Engineering Research Council, UK,
Natural Sciences and Engineering Research Council, Canada,
Israeli Ministry of Science,
Minerva Gesellschaft,
Japanese Ministry of Education, Science and Culture (the Monbusho) and a grant under the Monbusho International Science Research Program,
American Israeli Bi-national Science Foundation,
Direction des Sciences de la Matière du Commissariat à l'Energie Atomique, France,
Bundesministerium für Forschung und Technologie, FRG,
National Research Council of Canada, Canada,
A.P. Sloan Foundation and Junta Nacional de Investigação Científica e Tecnológica, Portugal.

References

[1] Particle Data Group, J.J. Hernandez *et al.*, Phys. Lett. **239B** (1990), pVI.14.

[2] B.C. Barish and R. Stroynowski, Phys. Rep. **157** (1988) 1.

[3] T.N. Truong, Phys. Rev. **D30** (1984) 1509.
F.J. Gilman and S.H. Rhie, Phys. Rev. **D31** (1985) 1066.
K.G. Hayes and M.L. Perl, Phys. Rev. **D38** (1988) 3351.

[4] ALEPH Collaboration, D. Decamp *et al.*, CERN-PPE/91-186 (1991), submitted to Z.Phys. C.
L3 Collaboration, B. Adeva *et al.*, Phys. Lett. **B265** (1991) 451.

[5] ARGUS Collaboration, H. Albrecht *et al.*, DESY/91-084, July 1991.

[6] K. Riles, *Proceedings of Particles and Fields 91, Vol. 1*, Univ. of British Columbia, Vancouver, August 1991.

[7] HRS Collaboration, S. Abachi *et al.*, Phys. Rev. **D40** (1989) 902.

[8] CELLO Collaboration, H.J. Behrend *et al.*, Phys. Lett. **B222** (1989) 163.

[9] OPAL Collaboration, K. Ahmet *et al.*, Nucl. Instr. and Meth. **A305** (1991) 275.

[10] J. Allison *et al.*, Comp. Phys. Comm. **47** (1987) 55;
D. R. Ward, *Proceedings of the MC'91 Workshop*, NIKHEF, Amsterdam, 1991.
J. Allison *et al.*, CERN-PPE/91-234 (1991), to be published in Nucl. Instr. and Meth.

[11] OPAL Collaboration, G. Alexander *et al.*, Z. Phys. **C52** (1991) 175.

[12] OPAL Collaboration, G. Alexander *et al.*, Phys. Lett. **B266** (1991) 201.

[13] S. Jadach, J.H. Kuhn, and Z. Was, Comp. Phys. Comm. **64** (1991) 275; TAUOLA.
S. Jadach, B.F.L. Ward, and Z. Was, Comp. Phys. Comm. **66** (1991) 276;
KORALZ, Version 3.7.

[14] M. Böhm, A. Denner and W. Hollik, Nucl. Phys. **B304** (1988) 687;
F.A. Berends, R. Kleiss, W. Hollik, Nucl. Phys. **B304** (1988) 712; BABAMC.

[15] T. Sjöstrand, Comp. Phys. Comm. 39 (1986) 347; JETSET.

[16] R. Bhattacharya, J. Smith, G. Grammer, Phys. Rev. **D15** (1977) 3267;
J. Smith, J.A.M. Vermaseren, G. Grammer, Phys. Rev. **D15** (1977) 3280.

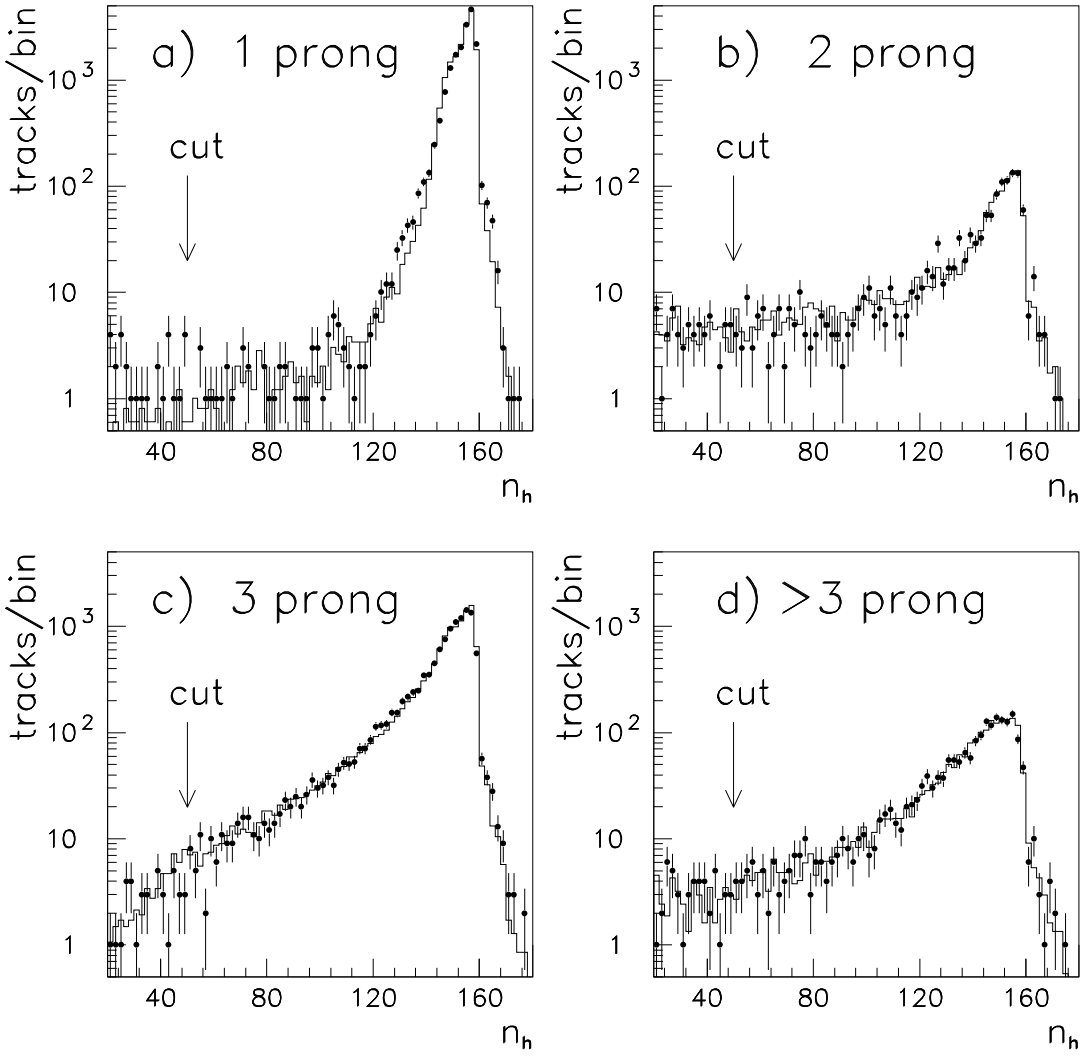

FIGURE 1: The number of jet chamber hits per track, n_h, is plotted for jets with a) one, b) two, c) three and d) more than three associated charged tracks. The points correspond to the data while the histogram shows the Monte Carlo prediction. The requirement that $n_h \geq 50$ for "good" charged tracks is shown.

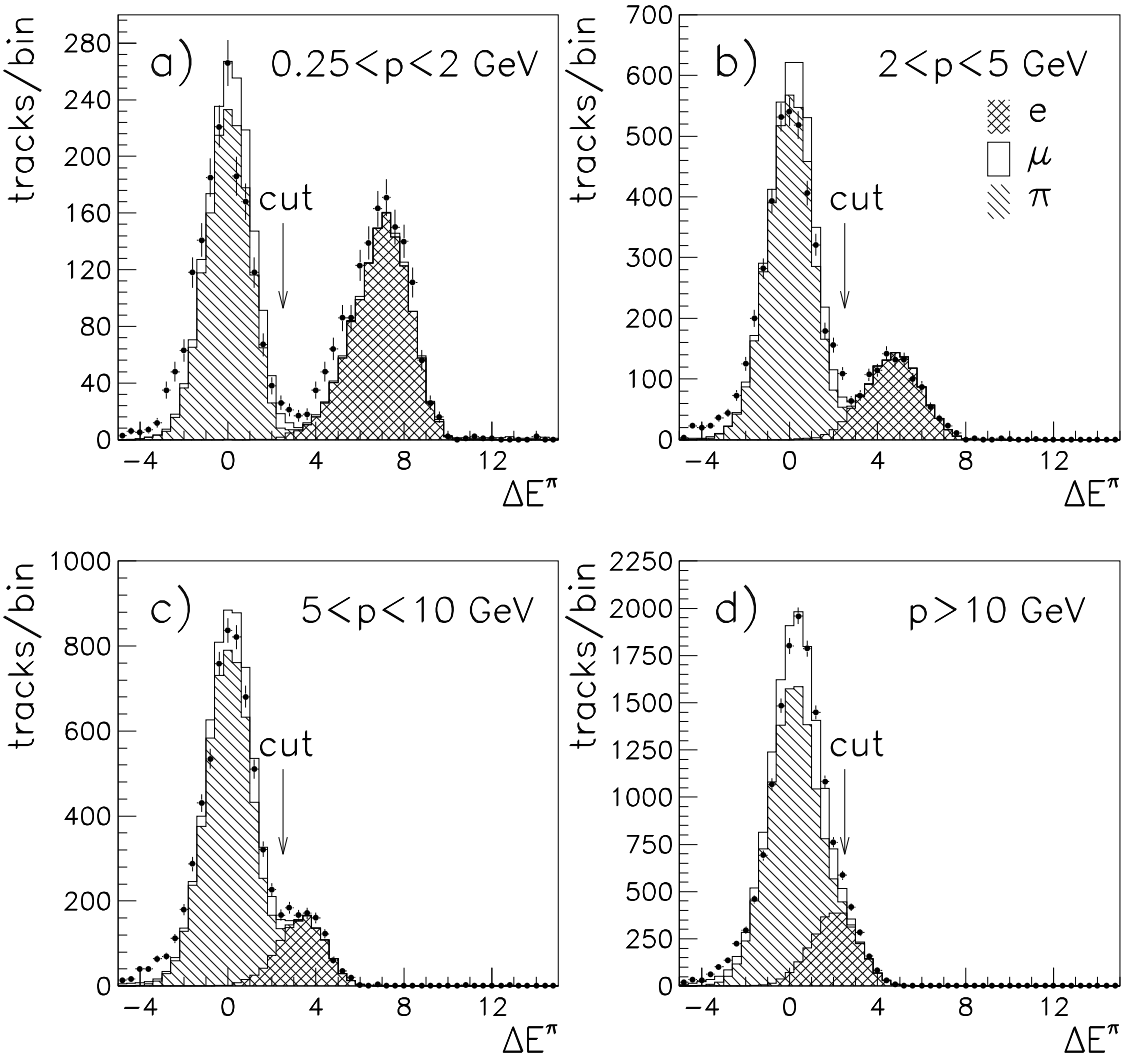

FIGURE 2: Distributions of the difference between track energy loss dE/dx and the expected energy loss for an pion, ΔE^{π}, for tracks with 20 or more jet chamber hits used in the dE/dx measurement and momentum a) between 0.25 and 2 GeV, b) between 2 and 5 GeV, c) between 5 and 10 GeV and d) above 10 GeV. The points with error bars represent the data while the open histogram shows the Monte Carlo prediction for electrons, muons and pions normalised to the number of τ pair events after background subtraction. The cut at $\Delta E^{\pi} > 2.5$ used to identify electrons is shown.

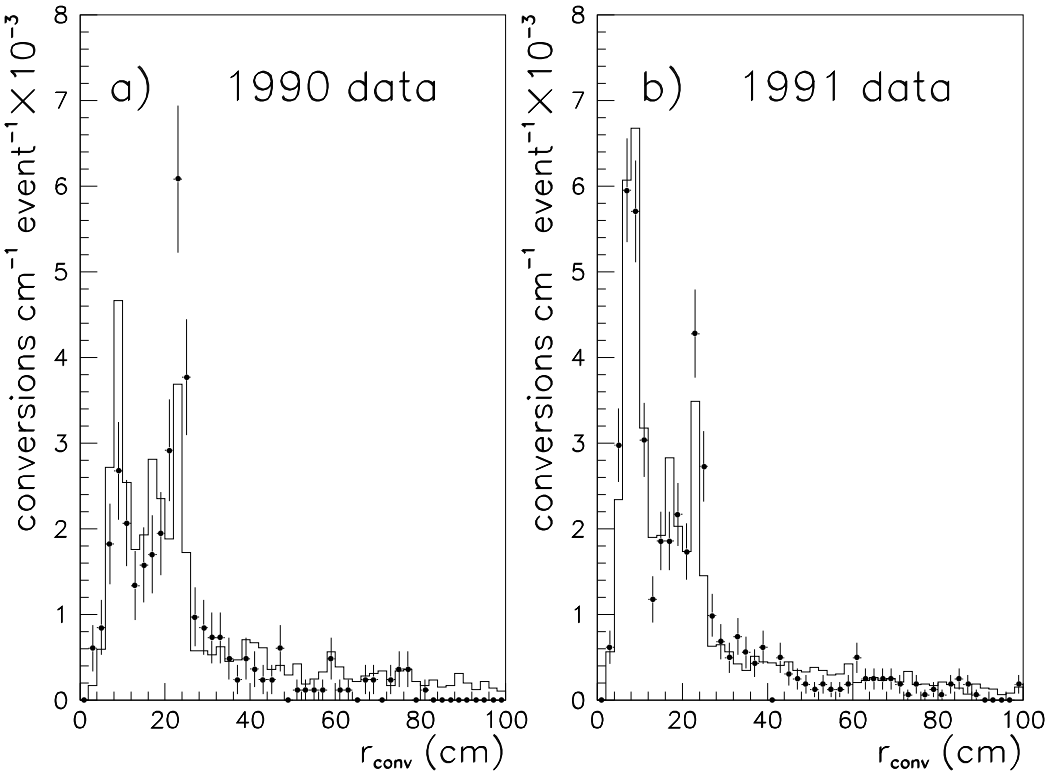

FIGURE 3: The distance from the beam axis for reconstructed photon conversions for data taken a) in 1990 and b) in 1991. The points represent the data while the open histogram shows the Monte Carlo prediction normalised to the number of τ pair events after background subtraction.